Hierarchical Climate Zone as a tool for spatial planning – Case study of Wuhan, China

[1]Jiong Wang, *Qingming Zhan and Yinghui Xiao

Abstract

The Koppen Climate Classification system is one of the examples dissecting global climate process into uniform zones. Due to the fractal structure of geographic phenomenon, the classification of climate zones may be applied at different scales to promote further understanding of climate system at the human-environment interface. This research presents a workflow of classifying climate zones by using meteorological sensitive indicators. The research recommends the zones should be in hierarchical manner such that planning and design at different levels can benefit from the framework. In the case study, the research begins by investigating the proper scale of study by choosing the appropriate pixel size. Then an illustration of the workflow is presented by using 6 meteorological sensitive indicators derived by using remotes sensing and geographic information tools. Instead of using empirical standards, the *K*-mean clustering is applied to leverage the intrinsic structure of the data. Both intensive and less built environment are classified to different urban and rural climate zones. The classification shows that the zones possess distinctive climate properties.

Jiong Wang • Qingming Zhan (Corresponding author) • Yinghui Xiao
School of Urban Design, Wuhan University, 8 Dong Hu Nan Lu, Wuhan 430072, China
Email: jiongwang@whu.edu.cn

Qingming Zhan. Email: qmzhan@whu.edu.cn

Yinghui Xiao.
Email: 344019209@qq.com

1. INTRODUCTION

One of the significant weaknesses of current research of microclimate is the lack of standards. The weakness eliminates the quantitative measurement of meteorology phenomenon at local scale and the development of local meteorological research such as urban climate (Stewart and Oke 2009; Stewart 2011). Most planning and design concepts are restricted by lacking quantitative standards to mitigate and adapt climate uncertainties (Grimmond et al. 2010; Stone, Vargo, and Habeeb 2012; Farr 2012). The weakness is quite intuitive in the study of temperature patterns and variations at local scale (Arnfield 2003). The Urban Heat Island (UHI) is conventionally measured as the temperature difference between the sample points representing urban and rural areas respectively. The definition of UHI brings several uncertainties when the dynamics of microclimate and the heterogeneity of land use types are considered (Anderson et al. 2008; Stewart and Oke 2009). The pattern of temperature is the result of the intrinsic complex interactions between background meteorology and land surface specifications (De Kauwe et al. 2013; Zhao et al. 2014), where selection of the representative measurements is ultimately restricted (Stewart 2011). First of all, the location of the study area and the background synoptic weather condition makes the UHI from a fixed urban-rural observational pair a non-static measurement. Similar urban-rural configuration located at different region of the globe may bring distinctive UHI behavior because of the background climate (De Kauwe et al. 2013). Second, the configuration of the land surface is by no means to be static in terms of the seasonal or even daily dynamics of water bodies and vegetation, as well as the thermal response of the land surface in different seasons (Oke 1988, 1997; Van De Kerchove et al. 2013). The urban-rural dichotomy is no longer enough to characterize the land surface heterogeneity of cities around the world today (Stewart 2011). The research of any other microclimate is without exception, such as the studies of airflow, humidity, pollution and precipitation. The Local Climate Zone (LCZ) is proposed such that the study of microclimate can be set into a standard background. Instead of using UHI as the indicator of temperature difference between areas with different land surface specification, the framework of LCZ recommend that the land surface should be classified into zones quantitatively according to their meteorological responses. The classification indicators include the surface material and morphological properties. This can be further defined according to the surface configuration of natural and built environment, such as relief, vegetation, water coverage, Impervious Surface Fraction (ISF) and Pervious Surface Fraction (PSF), building density,

roughness, Sky View Factor (SVF), as well as surface albedo. In this way, take temperature for example; the thermal response of each LCZ is measured to reflect one of the climate patterns of a certain area. The temperature and thermal property of a place is thus distinguished from the one of another place by the difference of LCZ temperature instead of UHI. Since the classification of the LCZs is based upon a set of indicators which reflects certain meteorological property of the study area, the LCZs provide a configuration of climatic ingredients of the area and depict how the climatic patterns of the area locally.

The LCZ is a framework proposed recently, it has been validated through circling places with radius of hundreds of meters in few cities (Stewart, Oke, and Krayenhoff 2014). The application of the concept is rarely found. Szeged, Hungary, began to apply the framework to the whole city in 2014 (Lelovics et al. 2014). More applications and tests of the framework are needed to bring insights of the dynamics of local climate at local scale (Middel et al. 2014). Leveraging the concept of the LCZ, this research intends to classify the target city into climate zones with homogenous climate response. The research provides a workflow of classification of climate zones. The research applies the idea to a whole city and the results can be used as a standard to distinguish climate behavior of the city at local scale. Considering the extent of study, employing geographic information and remotes sensing tools is more feasible than field study and measurement (Li et al. 2013). As a workflow, several issues are addressed through the classification process. At the beginning, the scale of the study which determines the size of pixel used is identified. The indicators used are then illustrated. The investigation of climatic response of the LCZs is also recommended.

2. DATA and METHODOLOGY

In this research, Wuhan, China, is selected for case study. Wuhan is the fifth most populous city of the nation. Located in central China, the city possesses humid subtropical climate, with oppressive humid summer. Wuhan is characterized by its heterogeneity of land use type, which differentiates itself from the cities in other studies. As shown in Fig.2.1, the extent of the study area is defined by a 45×36km rectangle, which covers the entire urban area of Wuhan and reaches into the rural surrounding by few kilometers, the coordinates of the upper-left and lower-right corners are “30°43′53″N, 114°4′49″E” and “30°24′0″N, 114°32′34″E” respectively. The selection of the extent is sufficient to characterize the land composi-

tion of the city. The L1T product with the resolution of 30 meters captured by Landsat-7 ETM+ is employed. The images selected are acquired on May 17th, 2012. The two images are used in order to examine whether seasonal or temporal dynamics exists.

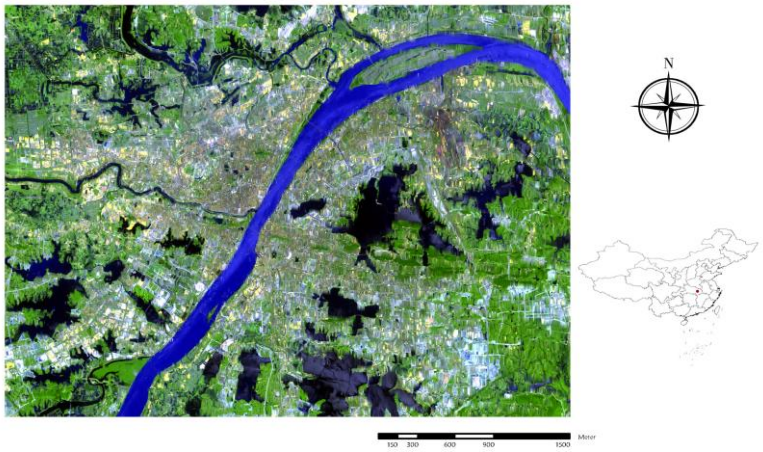

Fig. 2.1. Study Area represented by false color image. SWIR2, NIR, and Green bands of Landsat ETM+ are combined to highlight the land surface heterogeneity of built environment, vegetation and water bodies.

2.1 Resolution

In general, research results with geographic specifications are substantially impacted by the extent of study, the spacing of sampling, the measurement scale of observation, the scale of underlying phenomenon or process, and the scale of cartography. Specifically, the observational scale selected by researchers and the operational scale of the phenomenon is of great concern. Explore the proper scale before classification is made possible by seeking the *"break point"* (Lam and Quattrochi 1992) in *(semi-)variogram* since any phenomenon with spatial dimension is inherently governed by the Tobler's First Law (TFL) of Geography (Miller 2004). The plot of semivariance as a function of lag is referred as *(semi-)variogram*. It measures the difference between the LST as variables observed at various locations, and how the differences vary against distances between samples in a pair, it is calculated through:

$$\gamma(h) = \frac{1}{2N(h)} \sum_{i=1}^{N(h)} (t_i - t_{i+h})^2 , \quad (2.1)$$

where $\gamma(h)$ is the semivariance between two LST observation samples t_i and t_{i+h} in a pair with lag h. $N(h)$ is the number of sample pairs with lag h.

2.2 Indicators

Indicators are selected to reflect the meteorological properties of the land surface factors. The proposed indicators are shown in Table 2.1. In this research, only part of the indicators is used to illustrate the classification process.

Table 2.1. Indicators used for LCZs Classification

No.	Indicators	Definition	Meteorological Implication	Data Source	Resolution
1	Sky View Factor (SVF)	The fraction of sky visible from a certain point of land surface. Value range is [0,1].	Response actively to solar radiation and heat dissipation.	Building Survey of Wuhan, 2012	500m
2	Building Surface Fraction (BSF)	The fraction of building footprint in a certain land unit. Value range is [0,1].	Relates to surface run-off and moisture.	Building Survey of Wuhan, 2012	500m
3	Impervious Surface Fraction (ISF)	Fraction of impervious surface. Value range is [0,1].	Relates to surface run-off and moisture.	Landsat ETM+	500m
4	Pervious Surface Fraction (PSF)	Fraction of pervious surface such as vegetation and water. Value range is [0,1].	Relates to surface run-off and moisture.	Landsat ETM+	500m
5	Vegetation Index (VI)	Coverage of vegetation. Value range is [0,1].	Relates to energy and water transitions.	Landsat ETM+	500m
6	Water Index (WI)	Coverage of water bodies. Value range is [0,1].	Relates to energy and water transitions.	Landsat ETM+	500m

7	Height of Roughness Elements (HRE)	Height of constructions and natural relief. Value range is [0,MaximumHeight].	Affects the airflow and heat dissipation within urban area.	Building Survey of Wuhan, 2012	500m
8	Terrain Roughness Class (TRC)	Classification of roughness height. Value range is int[1,8].	Same as the above	Building Survey of Wuhan, DEM, 2012	500m
9	Digital Elevation /Surface Model (DSM)	Depicts the morphological property of relief. Value range is [MinimumHeight, MaximumHeight].	Same as the above	DEM, 2012	500m
10	Surface Admittance (SAD)	The capability to absorb and emit energy. It is the ratio between the two. Value range is [0,1].	The efficiency of transmitting energy.	Landsat ETM+	500m
11	Surface Albedo (SA)	The overall reflectance. It is the integration of reflectance in all directions.	The efficiency of reflect short wave radiation.	Landsat ETM+	500m

Fig. 2.2 also gives a snapshot of ISF and PSF as an example indicator. The ISF and PSF are considered as very important indicators for their relationship to energy, thermal, moisture transition, and surface run-off (Schwarz et al. 2012). They are obtained by applying the Vegetation-Impervious Surface-Soil (V-I-S) model (Ridd 1995).

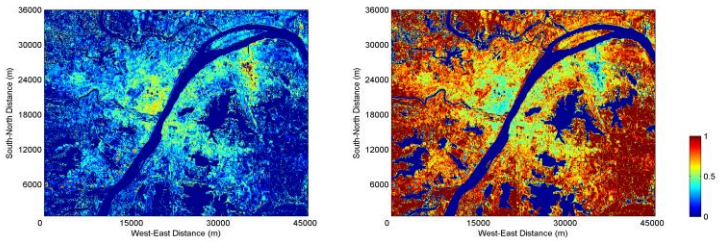

Fig. 2.2. The Impervious and Pervious Surface Fractions (ISF, PSF) of Wuhan on May 17th, 2012. The (a) ISF and (b) PSF are within the range of [0, 1].

The model assumes that the land cover types are essentially comprised of high, low albedo surfaces, as well as vegetation and soil. For

each pixel, the reflectance or the spectra is a linear combination of the spectrum of each land surface type. The partitioning of the compositions of land cover types is carried out through analyzing the mixture of spectrum at the pixel level, which is referred as Spectral Mixture Analysis (SMA). Thus for each band b, the reflectance of a single pixel follows:

$$R_b = \sum_{i=1}^{N} f_i R_{bi} + e_b \,, \tag{2.2}$$

where R_b is the reflectance of band b. R_{bi} is the reflectance of land type i within a pixel, this reflectance is assumed to be the spectra of a pure pixel of this certain land type called endmember. f_i is the fraction of the land type at the pixel level representing high albedo, low albedo, soil, and vegetation, and e_b is the intrinsic residual of the model.

The impervious fraction, for example, can be obtained through:

$$f_{im} = f_{low} + f_{high} \,, \tag{2.3}$$

where f_{low} and f_{high} are fractions of low and high albedo surfaces respectively.

2.3 Classification

The indicators are considered as properties of a certain area of the land surface, which means for each pixel, its properties can be taken as a multi-dimensional vector. In this situation, the *K*-means clustering is applied for the reason that such classification approach utilizes the intrinsic structure of the data as opposed to artificially partition the observations by using empirical values. In this study, the pixels can be viewed as n observations, and for each observation the properties is an d dimensional vector $\mathbf{p}$. All the pixels are in a d dimensional space $(\mathbf{p}_1, \mathbf{p}_2, ..., \mathbf{p}_n)$. The *K*-means clustering separates the pixels into k sets to minimize the within-cluster sum of squares. Thus it tries to find

$$\arg\min \sum_{i=1}^{k} \sum \left\| \mathbf{p} - \boldsymbol{\mu}_i \right\|^2 \,, \tag{2.4}$$

where $\boldsymbol{\mu}_i$ is the mean of cluster i.

3. RESULTS

3.1 The Scale of Study

The land surface temperature (LST) is selected as one of the meteorological phenomenon to investigate the operational scale that can be used in this research. The LST not only represents the thermal response of the land surface composition, but also contains the energy balance and airflow patterns implicitly within the study area. The 1-dimensional analysis is established on two series of LST measurements, which are the west-east (horizontal) and south-north (vertical) cross-sections through the center of the study area. The empirical semivariance and covariance of the 1-dimensional measurements are generated for May 17th, 2012.

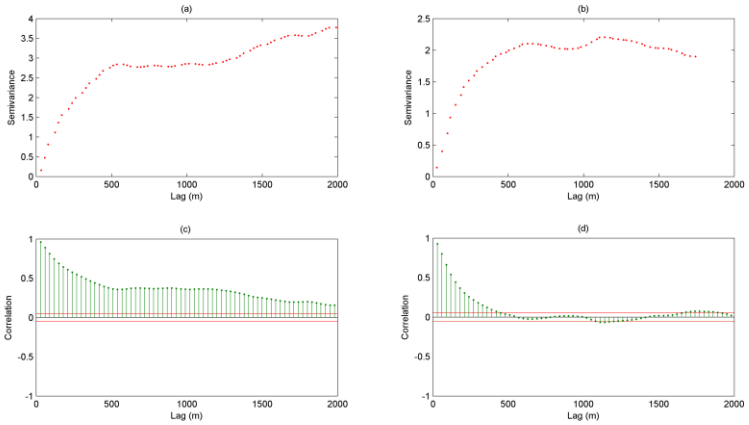

Fig. 3.1. The Variogram and correlogram of a random cross-section of the LST. The (a) Semivariance and (b) correlation are plotted with first 2000m lag distance.

In the case of the measurements from January, Fig. 3.1(a) shows the semivariance grows smoothly within the lag distance range of 0 to 500 meters, meaning that the difference and the distance of a measurement pair increase accordingly. The first discernable "*break points*" appears when the semivariance levels off beyond 500m. This critical point indicates that similar measurements are clustered at the scale of around 500m, and resolution of 500m is appropriate to represent a homogenous land surface unit. In Fig. 3.1(b), the first "*break point*" also appears around the 500m lag distance, again indicating the level of operational scale. Fig. 3.1(c) and 3.1(d)

plot the corresponding correlogram of Fig. 3.1(a) and Fig. 3.1(b) for validation. The results imply that resolution around 500m is appropriate in studying the climate phenomenon in this research.

3.2 The Classification of Climate Zones

While the proper scale is identified as 500m, the classification is based upon this resolution. In this research, only 6 indicators are used for illustration. By applying the *K*-means clustering for sufficient of repetitions, 5-category classification is found to be best suited for the study area, which means the classification is neither complicate nor simple. Fig. 3.2 is an illustration of the classification. The shape of the climate zones outlines the distribution of built environment meaning that artificial manipulation of land surface imposes significant impacts on climate. Water bodies are distinguished from the rest of the land surface. The areas with relatively intensive urban development are classified as Urban A and B, while those ones with less artificial intervention are classified as Rural A and B.

It is interesting to find that climate zone Urban A shows up not only around the urban core, but also at the edge of the urban area. Superficially, the climate zone Urban A in urban core area and the one at the north-east urban peripheral differentiate from each other in terms of their function. The downtown area is characterized by high-rise business and office buildings, while the one to the north-east is characterized by large clusters of low factory building and industrial power plants. However, their climate response is quite similar due their combined properties of ISF, SVF, NDVI and so on. And it is intuitive to assume that downtown area and factories are both sensitive to environment and climate.

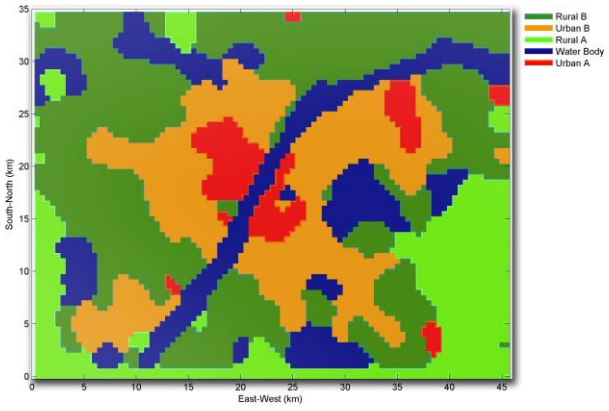

Fig. 3.2. Classification of climate zones of Wuhan.

The classification is sufficient to represent the inter-class discrepancies and maintain the coherence within each one of cluster. Table 3.1 shows how each class of climate zones responses to the environment. Urban A and B are characterized by high ISF and low PSF which implies that these areas are sensitive to solar radiation as well as surface run-off. The low NDVI in these areas also indicates that insufficient vegetation cover may exacerbate the thermal response of downtown Wuhan. In addition, the intensive development in Urban A and B makes the SVF value to reach to the lower end of the range, this can be another factor that cities have distinctive radiation and energy balance in terms of their geometric structure. The climatic reaction of the zones weakens as artificial intervention decreases. Rural A can be considered as the transition between Urban B and Rural B, it combines newly developed high-rise communities and cropland. Rural B is more environmental-friendly as it is composed of cropland and other vegetations, yet communities are scattered in the area.

Table 3.1. The meteorological sensitivity of climate zones

Category		Albedo	ISF	PSF	NDVI	NDWI	SVF	Percentage of Study Area (%)
Urban	Urban A	[0.1539~0.3434]	[0.12963~0.7314]	[0.0000~0.8713]	[-0.1472~0.3235]	[-0.2629~0.0920]	[0.1964~0.9708]	5.78
	Urban B	[0.1718~0.3491]	[0.0537~0.5672]	[0.0008~0.9969]	[-0.0702~0.3863]	[-0.2571~0.1826]	[0.3224~0.9896]	21.00
Rural	Rural A	[0.0973~0.3552]	[0.0000~0.2298]	[0.3958~0.9997]	[-0.2585~0.6725]	[-0.3002~0.7496]	[0.5872~1.0000]	15.84
	Rural B	[0.1845~0.2945]	[0.0000~0.3489]	[0.4346~0.9973]	[-0.0762~0.6067]	[-0.2927~0.1174]	[0.8673~1.0000]	33.58
Others	Water Body	[0.0872~0.2977]	[0.0000~0.1969]	[0.7466~0.9969]	[-0.2717~0.0013]	[-0.0271~0.8533]	[0.8730~1.0000]	23.80

Finally, an illustration photo set is shown in Fig. 3.3 to provide intuitive understanding of each of the climate zone profiles. Fig. 3.3(a) show the climate zone Urban A is occupied by intensive development of urban constructions, it combines high-rise office buildings, residential area, downtown square with large fraction of impervious surface. Such configuration corresponds to the information indicated in Table 2. Fig. 3.3(b) indicates that climate zone Urban B is mainly composed of residential communities and schools with lower development intensity, which is discernable from the lower density of the building clusters. The increase of SVF shown in Table 3.1 is evidence. Rural A and Rural B show increase of both vegetation cover and SVF which goes along with decrease of ISF.

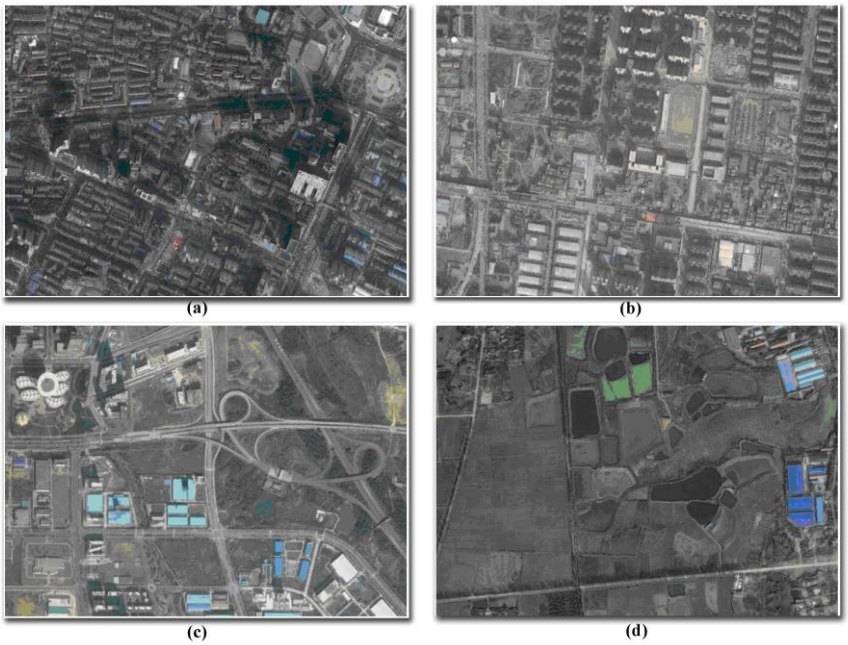

Fig. 3.3. Sample photos of climate zone profiles. (a) Urban A, (b) Urban B, (c) Rural A, and (d) Rural B.

4. DISCUSSION and CONLUSION

While synoptic and meso-scale climate zones quantify the operational concept of measuring, mitigating and adapting natural influences and processes upon human society, this research recommend to build local scale climate zones to form a hierarchical climate sensitive zoning system. Builds upon the concept of Urban Climate Zone and Local Climate Zone initiated by Oke's (2011) research team, the research apply the idea to an entire city as opposed to sample land units in previous studies. Several meteorological indicators are employed to reflect the climate property of land surface factors, such as the SVF, ISF and NDVI. The climate properties are contained in the indicators implicitly, for instance, the SVF may reflect the geometric pattern of building clusters in an area which in turn determines the thermal response to the solar radiation and airflow, whereas the ISF is an indicator sensitive to both energy balance and surface run-off. Using

these indicators means to accept the empirical understanding of the relationship among the indicators and certain climatic phenomenon.

Two issues are addressed in this study. First, any type of climate study possesses geographic dimension, which means that the scale of study imposes significant effects on the results (Sobrino et al. 2012). In this research, the idea of "*break points*" in variogram is employed to identify the proper resolution for this study, in other words, the operational scale. Different operational scale may be found when the study extent or sampling techniques differ. Second, by leveraging the framework initiated by Oke and Stewart, one should be careful when classification is conducted. The original LCZ framework provide empirical standard for classification of land surface composition, the completeness of the indicators in the original study is yet to be sufficient to character cities around the world. In this study, the *K*-means clustering is applied to follow the structure and pattern of the data, in this way; the classes are assigned according the data itself as opposed to standards found in other cities.

Further research is highly recommended in two domains. On one hand, the completeness of indicators means to characterize the climatic or meteorological property of surface factor with enough details. Besides thermal and airflow pattern, others such as humidity, moisture and pollution are also expected to be captured by the indicators. On the other hand, the study of climate zones is by no means to by static. While the zones may stay as it is for a certain period of time, the energy and flows keep changing and transitioning at any time and location (Lowry 1977). While the Koppen Climate Zones at the global scale provide the standard to study the dynamics of climate at synoptic scale, the dynamics of the zones at local scale remains uncertain. One may benefit from the framework of global climate study routines and extend the framework through space and time hierarchically.

ACKNOWLEDGEMENT

This research is supported by the National Natural Science Foundation of China (No.: 51378399).

References

Anderson, MC, JM Norman, WP Kustas, R Houborg, PJ Starks, and N Agam. 2008. "A thermal-based remote sensing technique for routine

mapping of land-surface carbon, water and energy fluxes from field to regional scales." *Remote Sensing of Environment* 112 (12):4227-41.

Arnfield, John. 2003. "Two Decades of Urban Climate Research: A Review of Turbulence Exchanges of Energy and Water, And the Urban Heat Island." *Int. J. Climatol* 23:26. doi: 10.1002/joc.859.

De Kauwe, Martin G, Christopher M Taylor, Philip P Harris, Graham P Weedon, and Richard J Ellis. 2013. "Quantifying land surface temperature variability for two Sahelian Mesoscale Regions during the wet season." *Journal of Hydrometeorology* 14 (5):1605-19.

Farr, Douglas. 2012. *Sustainable urbanism: urban design with nature*: John Wiley & Sons.

Grimmond, CSB, M Roth, TR Oke, YC Au, M Best, R Betts, G Carmichael, H Cleugh, W Dabberdt, and R Emmanuel. 2010. "Climate and more sustainable cities: Climate information for improved planning and management of cities (producers/capabilities perspective)." *Procedia Environmental Sciences* 1:247-74.

Lam, Nina Siu‐Ngan, and Dale A Quattrochi. 1992. "On the Issues of Scale, Resolution, and Fractal Analysis in the Mapping Sciences*." *The Professional Geographer* 44 (1):88-98.

Lelovics, E, J Unger, T Gál, and CV Gál. 2014. "Design of an urban monitoring network based on local climate zone mapping and temperature pattern modelling." *Clim Res* 60:51-62.

Li, Zhao-Liang, Bo-Hui Tang, Hua Wu, Huazhong Ren, Guangjian Yan, Zhengming Wan, Isabel F. Trigo, and José A. Sobrino. 2013. "Satellite-derived land surface temperature: Current status and perspectives." *Remote Sensing of Environment* 131:14-37.

Lowry, William P. 1977. "Empirical estimation of urban effects on climate: a problem analysis." *Journal of applied meteorology* 16 (2):129-35.

Middel, Ariane, Kathrin Häb, Anthony J Brazel, Chris A Martin, and Subhrajit Guhathakurta. 2014. "Impact of urban form and design on mid-afternoon microclimate in Phoenix Local Climate Zones." *Landscape and Urban Planning* 122:16-28.

Miller, Harvey J. 2004. "Tobler's first law and spatial analysis." *Annals of the Association of American Geographers* 94 (2):284-9.

Oke, TR. 1988. "Street design and urban canopy layer climate." *Energy and buildings* 11 (1):103-13.
———. 1997. "Urban climates and global environmental change." *Applied Climatology: Principles & Practices. New York, NY: Routledge*:273-87.

Ridd, Merrill K. 1995. "Exploring a VIS (vegetation-impervious surface-soil) model for urban ecosystem analysis through remote sensing: comparative anatomy for cities†." *International Journal of Remote Sensing* 16 (12):2165-85.

Schwarz, Nina, Uwe Schlink, Ulrich Franck, and Katrin Großmann. 2012. "Relationship of land surface and air temperatures and its implications for quantifying urban heat island indicators—An application for the city of Leipzig (Germany)." *Ecological Indicators* 18 (0):693-704. doi: http://dx.doi.org/10.1016/j.ecolind.2012.01.001.

Sobrino, JA, R Oltra-Carrió, G Sòria, R Bianchi, and M Paganini. 2012. "Impact of spatial resolution and satellite overpass time on evaluation of the surface urban heat island effects." *Remote Sensing of Environment* 117:50-6.

Stewart, Iain D. 2011. "A systematic review and scientific critique of methodology in modern urban heat island literature." *INTERNATIONAL JOURNAL OF CLIMATOLOGY* 31 (2):200-17.
Stewart, Iain D, TR Oke, and E Scott Krayenhoff. 2014. "Evaluation of the 'local climate zone'scheme using temperature observations and model simulations." *INTERNATIONAL JOURNAL OF CLIMATOLOGY* 34 (4):1062-80.

Stewart, Iain, and TR Oke. 2009. Newly developed "thermal climate zones" for defining and measuring urban heat island magnitude in the canopy layer. Paper presented at the Eighth Symposium on Urban Environment, Phoenix, AZ.

Stone, Brian, Jason Vargo, and Dana Habeeb. 2012. "Managing climate change in cities: Will climate action plans work?" *Landscape and Urban Planning*.

Van De Kerchove, Ruben, Stefaan Lhermitte, Sander Veraverbeke, and Rudi Goossens. 2013. "Spatio-temporal variability in remotely sensed land surface temperature, and its relationship with physiographic variables in the Russian Altay Mountains." *International Journal of Applied Earth Observation and Geoinformation* 20:4-19.

Zhao, Lei, Xuhui Lee, Ronald B Smith, and Keith Oleson. 2014. "Strong contributions of local background climate to urban heat islands." *Nature* 511 (7508):216-9.